

## Article

# Experimental Research on the Preparation of K<sub>2</sub>CO<sub>3</sub>/Expanded Vermiculite Composite Energy Storage Material

Dequan Zou, Xiangji Yue \*, Tianyi He, Jianan Ding and Dechun Ba

School of Mechanical Engineering and Automation, Northeastern University, Shenyang 110819, China; zoudequan1220@163.com (D.Z.); 1970264@stu.neu.edu.cn (T.H.); jnding@yeah.net (J.D.); dchba@mail.neu.edu.cn (D.B.)

\* Correspondence: yuexjneu@126.com

**Abstract:** Thermochemical adsorption energy storage is a potential energy utilization technology. Among these technologies, the composite energy storage material prepared by K<sub>2</sub>CO<sub>3</sub> and expanded vermiculite (EVM) shows excellent performance. In this paper, the influence of the preparation process using the impregnation method and vacuum impregnation method on K<sub>2</sub>CO<sub>3</sub>/EVM composite material is studied. The preparation plan is further optimized with the solution concentration and the expanded vermiculite particle size as variables. In the experiment, mercury intrusion porosimetry (MIP) is used to measure the porosity and other parameters. Additionally, with the help of scanning electron microscopy (SEM), the morphological characteristics of the materials are obtained from a microscopic point of view. The effects of different preparation parameters are evaluated by comparing the experimental results. The results show that the K<sub>2</sub>CO<sub>3</sub> specific gravity of the composite material increases with the increase of the vacuum degree, up to 70.440 wt.% (the vacuum degree is 6.7 kPa). Expanded vermiculite with a large particle size (3–6 mm) can carry more K<sub>2</sub>CO<sub>3</sub>, and content per cubic centimeter of K<sub>2</sub>CO<sub>3</sub> can be as high as 0.466 g.

**Keywords:** thermochemical energy storage; salt hydrates; vacuum impregnation; K<sub>2</sub>CO<sub>3</sub>; expanded vermiculite



**Citation:** Zou, D.; Yue, X.; He, T.; Ding, J.; Ba, D. Experimental Research on the Preparation of K<sub>2</sub>CO<sub>3</sub>/Expanded Vermiculite Composite Energy Storage Material. *Materials* **2022**, *15*, 3702. <https://doi.org/10.3390/ma15103702>

Academic Editor: Ricardo Alcántara

Received: 18 April 2022

Accepted: 19 May 2022

Published: 22 May 2022

**Publisher's Note:** MDPI stays neutral with regard to jurisdictional claims in published maps and institutional affiliations.

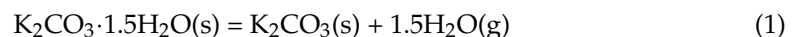


**Copyright:** © 2022 by the authors. Licensee MDPI, Basel, Switzerland. This article is an open access article distributed under the terms and conditions of the Creative Commons Attribution (CC BY) license (<https://creativecommons.org/licenses/by/4.0/>).

## 1. Introduction

The Intergovernmental Panel on Climate Change (IPCC) Special Report on Global Warming of 1.5 °C pointed out that reducing the average temperature rise from 2.0 °C to less than 1.5 °C will greatly reduce the risks of sea-level rise and urban high temperature [1]. Solar energy, as a renewable and clean energy source, used in building heating can help control global temperature rise [2]. However, the solar radiation is intermittent, and it has insufficient thermal energy supply in winter [3]. Therefore, the salt hydrates seasonal energy storage technology has become a hot spot in the field of energy utilization. The study found that the salt hydrate K<sub>2</sub>CO<sub>3</sub> has good reversibility, a low price and non-corrosiveness. Combining K<sub>2</sub>CO<sub>3</sub> and porous matrix expanded vermiculite (EVM) into a composite material can highlight the advantages of K<sub>2</sub>CO<sub>3</sub> [4,5].

For the K<sub>2</sub>CO<sub>3</sub> reaction equilibrium formula, see Formula (1). During the dehydration reaction, K<sub>2</sub>CO<sub>3</sub>·1.5H<sub>2</sub>O loses water and absorbs heat. During the hydration reaction, K<sub>2</sub>CO<sub>3</sub> combines with the water vapor medium to form a hydrate and release heat. The temperature required for K<sub>2</sub>CO<sub>3</sub> dehydration and hydration reaction is relatively low, which is suitable for medium- and low-temperature heat storage systems such as building heating [6].



There is a wide range of methods for preparing composites, among which the impregnation method is widely used. Yu et al. [7] immersed two kinds of silica gels with different average pore diameters in LiCl solution and separated them with a vacuum filter to obtain

LiCl/silica gel composite materials. They found that silica gels with larger pore sizes can carry more inorganic salts. Courbon et al. [8] prepared silica gel and LiBr composite adsorbent based on the multi-step incipient wetness method. Posern et al. [9] put Attapulgite granulate with a porosity of 74.3% in the mixed solution of  $\text{MgSO}_4$  and  $\text{MgCl}_2$ , and they found that the exothermic heat of the obtained composites increased with increasing  $\text{MgCl}_2$  content. Shere et al. [10] used the porous structure of zeolite to prepare mixed inorganic salt composites by impregnation. The experiment found that the energy storage density is maximum when the proportion of  $\text{MgCl}_2$  and  $\text{MgSO}_4$  is 50%. Chan et al. [11] immersed the zeolite in 46 wt.%  $\text{CaCl}_2$  solution and filtered it after 24 h to obtain a  $\text{CaCl}_2$ /zeolite composite material, in which the Ca content reached 41.5 mol%. Grekova et al. [12] used the impregnation method to immerse the EVM which had been dried for 16 h in the LiCl solution and then dried again at 160 °C to obtain a LiCl/EVM composite with a salt content of 59 wt.%. In order to prevent particle agglomeration and improve mass transfer, Veselovskaya et al. [13] soaked the EVM matrix in the  $\text{BaCl}_2$  aqueous solution to disperse the  $\text{BaCl}_2$  particles in the pores. Zhang et al. [14] immersed the dried EVM in  $\text{SrBr}_2$  solutions with different mass concentrations for 48 h. After testing multiple composite materials, they found that the  $\text{SrBr}_2$ /EVM composite material with a salt content of 63.02 wt.% is the best. With the development of the vacuum industry, the combination of vacuum technology and impregnation method forms a vacuum impregnation method, which provides a different impregnation environment for composite materials. Li et al. [15] prepared paraffin/EVM composites by vacuum impregnation and found that EVM can be loaded with up to 67% paraffin. Xu et al. [16] immersed paraffin in the lamellar gap of EVM based on a vacuum environment and learned that this composite material has excellent thermal stability according to the thermogravimetric analysis (TGA). Karaipekli et al. [17] also selected the vacuum impregnation method when immersing the eutectic mixture of fatty acids into the EVM, and measured that the maximum mass fraction of the impregnant can reach 40%.

Based on the preparation process of the impregnation method and the vacuum impregnation method, this paper uses EVM as the matrix to prepare  $\text{K}_2\text{CO}_3$ /EVM composite material. The influence of the operation process and the degree of vacuum on the  $\text{K}_2\text{CO}_3$ /EVM composite material during dipping is studied, and the feasibility of the preparation schemes are further discussed with the solution concentration and EVM particle size as variables. In addition, the distribution of  $\text{K}_2\text{CO}_3$  in the composite material is also described. The research results can provide a reference for the preparation of similar types of composite materials.

## 2. Materials and Instruments

In order to study the effects of operating procedures and differences in experimental variables, expanded vermiculite and anhydrous  $\text{K}_2\text{CO}_3$  are used to prepare  $\text{K}_2\text{CO}_3$ /EVM composite materials. Expanded vermiculite (EVM), which is obtained from vermiculite ore  $[(\text{Mg,Fe,Al})_8(\text{Al,Si})_4\text{O}_{10}](\text{OH})_2 \cdot 4\text{H}_2\text{O}]$  by thermal expansion method or chemical expansion method [18,19], has the characteristics of high porosity, low density, fire resistance, and is widely used in chemical, construction, metallurgy, environmental protection [20–23]. In this paper, two types of EVM are selected: E1 (3–6 mm) and E2 (0.4–0.8 mm). The appearance of EVM is shown in Figure 1. Anhydrous  $\text{K}_2\text{CO}_3$  is white granular, which crystallizes into white translucent crystals after hydration reaction. In this experiment, analytically pure anhydrous  $\text{K}_2\text{CO}_3$  is used.

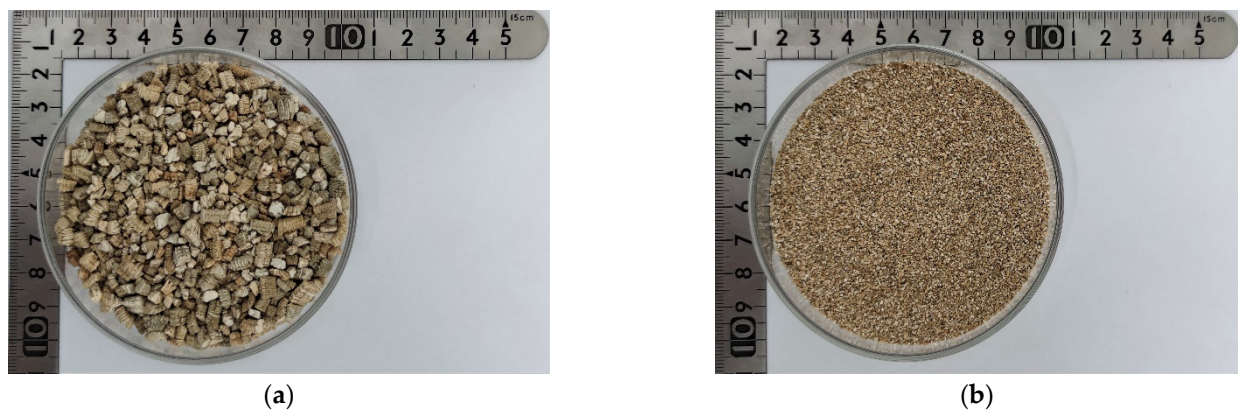


**Figure 1.** The appearance of the EVM. (a) E1 (3~6 mm); (b) E2 (0.4~0.8 mm).

Mercury intrusion porosimetry (MIP, AutoPore IV 9500) is used to measure the EVM of two particle sizes to obtain EVM porosity, pore size and other parameters. Take about 0.05 g of the EVM sample dried at a high temperature into the dilatometer, seal and weigh it. The experimental pressure range is  $3.58\sim 2.27 \times 10^5$  kPa, and the data are collected and analyzed.

The  $K_2CO_3$ /EVM composite material preparation equipment is composed of a rotary evaporator, vacuum gauge, pressure transmitter, scroll vacuum pump and surge tank, as shown in Figure 2. The materials are mixed in the rotating bottle of the rotary evaporator, and the other devices provide different vacuum degrees according to the experimental requirements. In the process of preparing the composite material, an electronic balance is used for weighing, and its division value is 0.001 g.

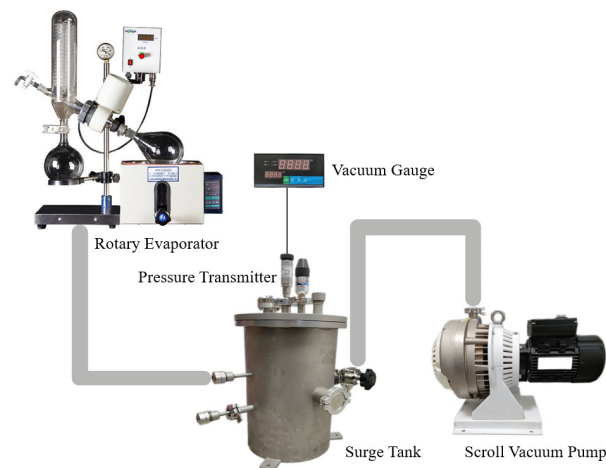


**Figure 2.** The  $K_2CO_3$ /EVM composite material preparation equipment.

A scanning electron microscopy (SEM, Hitachi S-4800) is used to observe the surface and cross-sectional microstructure of EVM and composite material to study the distribution of  $K_2CO_3$ . The sample after high-temperature drying is fixed on the sample stage with electrically conductive adhesive and is conductively treated by sputtering Pt. The sample is sent into the sample chamber and vacuumize to  $2 \times 10^{-3}$  Pa, and the SEM image is obtained under an acceleration voltage of 5.0 kV.

### 3. Preparation of Composite Material

According to the relevant descriptions of the above-mentioned preparation methods of composite materials, the preparation process of composite materials is designed based on the experimental objectives, as shown in Figure 3. When preparing the composite material

based on the impregnation method, the preparations such as drying the EVM, connecting the experimental equipment, and configuring the  $K_2CO_3$  solution with anhydrous  $K_2CO_3$  and deionized water are first carried out. Then put the  $K_2CO_3$  solution and EVM into a rotating bottle to mix and get impregnated. In the impregnation process, some samples added agitation and other operations. After the impregnation, the excess  $K_2CO_3$  solution was filtered with a screen and dried for the first time. Then the excess  $K_2CO_3$  was cleaned from the surface of the sample with deionized water. Sögütoglu et al. [24] believed that high-temperature heating can remove the  $KHCO_3$  impurities formed when  $K_2CO_3$  is stored in the air. Therefore, the composite material will finally be dried in a high-temperature environment of 120 °C for 8 h to remove moisture and possible  $KHCO_3$  impurities. When the composite material is dried, it is weighed using an electronic balance. The operation steps of the vacuum impregnation method in the preparation for impregnation and composite material processing stages are the same as those of the impregnation method. However, in the impregnation process, the vacuum impregnation method provides a certain degree of vacuum by twice vacuuming for the EVM to absorb the  $K_2CO_3$  solution. The salt content in the sample is expressed by the specific gravity  $\eta$  of  $K_2CO_3$  in the composite material. The larger the value of  $\eta$ , the more  $K_2CO_3$  contained in the unit mass sample, and the more conducive to energy storage. The calculation formula of  $\eta$  is:

$$\eta = \frac{m_{KE} - m_E}{m_{KE}} \times 100\% \quad (2)$$

wherein,  $m_{KE}$  is the mass of the composite material after drying, g;  $m_E$  is the mass of the EVM, g.

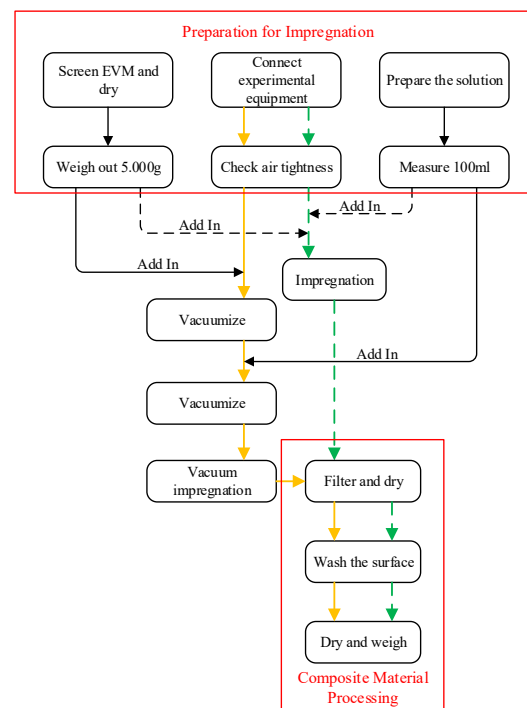


**Figure 3.** Composite material preparation process (---: impregnation preparation process; —: vacuum impregnation preparation process).

In this paper, three groups of composite materials are prepared, namely the KE1, KE2 and KE3 series, all of which are prepared with 5.000 g EVM and 100 mL  $K_2CO_3$  solution. The KE1 series of samples are used to study the influence of the operation and vacuum degree on the  $K_2CO_3$ /EVM composite material during impregnation, and to analyze the distribution of  $K_2CO_3$  with the help of SEM. The KE2 series samples are prepared by 0.4~0.8 mm EVM, and are compared with the KE1 series samples to study the

influence of the particle size of the EVM on the preparation of composite material. The KE3 series samples change the mass concentration of the  $K_2CO_3$  solution during the vacuum impregnation process and study the influence of the solution concentration on the  $K_2CO_3$  specific gravity and  $K_2CO_3$  distribution of the composite material. The main operations and formulas of each group of composite materials are shown in Table 1, where 1.12 g/mL solution is saturated  $K_2CO_3$  solution, and 0.125~0.750 g/mL solution is unsaturated  $K_2CO_3$  solution. Sample KE1-1 is the no. 1 sample prepared from 3~6 mmEVM and saturated  $K_2CO_3$  solution, and other samples are similar.

**Table 1.** The main operation and formula of composite materials.

Series	Sample No.	Main Operation	Operation during Impregnation	EVM Particle Size D/mm	Mass Concentration of $K_2CO_3$ Solution $\rho_k$ (g/mL)
KE1	KE1-1	Impregnation for 48 h	–	3~6	1.12
	KE1-2	Impregnation for 6 h	–		
	KE1-3	Impregnation for 6 h	Mix		
	KE1-4	Vacuum impregnation for 6 h	–		
	KE1-5	Vacuum impregnation for 6 h	Mix		
	KE1-6	Vacuum impregnation for 6 h	Mix + evaporated water		
KE2	KE2-2	Impregnation for 6h	–	0.4~0.8	1.12
KE3	KE2-4	Vacuum impregnation for 6 h	–	3~6	0.125~0.750
	KE3-1~4	Vacuum impregnation for 6 h	–		

## 4. Results and Discussion

### 4.1. The Specific Gravity of $K_2CO_3$

#### 4.1.1. Operation

In order to seek an ideal preparation process, in other words, to prepare composite material with high  $K_2CO_3$  specific gravity in the shortest time, there are 6 different schemes being designed for comparison. The specific data are shown in Table 2 among which KE1-1~KE1-3 are prepared by the impregnation method, and the KE1-4~KE1-6 samples are prepared by the vacuum impregnation method.

**Table 2.** KE1 series sample data.

Sample No.	KE1-1	KE1-2	KE1-3	KE1-4	KE1-5	KE1-6
Vacuum degree (absolute pressure) $P_{abs}$ /kPa	101.2	101.2	101.2	6.7	10.0	8.5
Quality after drying $m_{KE}$ /g	10.081	10.621	10.483	16.915	15.532	16.799
$K_2CO_3$ accounts for the specific gravity of composite material $\eta$ /wt.%	50.402	52.923	52.304	70.440	67.808	70.236

Table 2 shows that the salt mass carried by the KE1-4~KE1-6 samples is more than twice the mass of the EVM, resulting in the specific gravity of  $K_2CO_3$  in the composite material as high as 70.440 wt.%, which is about 20 wt.% higher than the three samples prepared by the impregnation method. It can be seen that the vacuum degree is very beneficial to increase the salt content of the composite material. Comparing the samples of KE1-1~KE1-3, it is found that the specific gravity of  $K_2CO_3$  does not change significantly, though the impregnation time of KE1-1 is 48 h and KE1-3 has a stirring operation. The  $\eta$  values of the three samples prepared by the vacuum impregnation method are all around 70 wt.%, and the increased operation of stirring and evaporating water does not have a great impact on the composite material. It can be seen from the above results that vacuum is the main factor to increase the specific gravity, and the use of vacuum impregnation can obtain composite material with high  $K_2CO_3$  specific gravity in a relatively short period of time.

### 4.1.2. Vacuum Degree

The vacuum degree is the main influencing factor in the preparation of composite material, so the relationship between its numerical value and the specific gravity of  $K_2CO_3$  becomes extremely important. The graph of the specific gravity of  $K_2CO_3$  with the vacuum degree is shown in Figure 4. The data of each point in the figure are obtained based on the vacuum impregnation method (KE1-4 sample preparation process). Figure 4 shows that when the vacuum degree is higher than 60 kPa, as the vacuum degree decreases (the preparation pressure increases), the specific gravity of  $K_2CO_3$  in the composite material shows a decreasing trend. When the preparation pressure exceeds about 60 kPa, the vacuum environment will not greatly promote the absorption of  $K_2CO_3$  solution by the EVM, and the specific gravity of  $K_2CO_3$  is stable at about 53 wt.%.

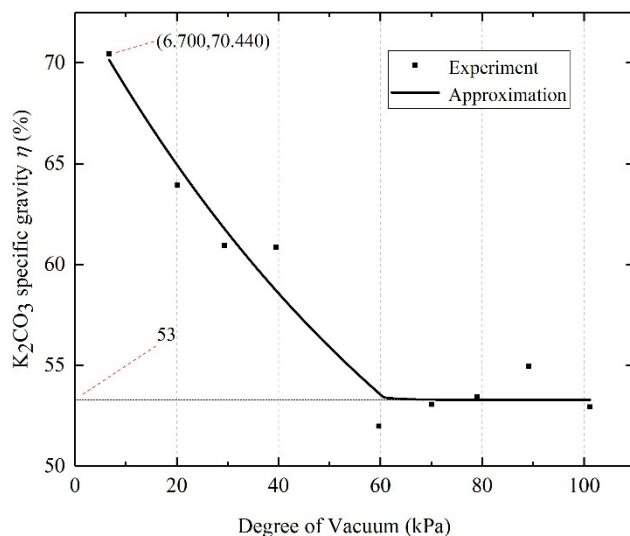


Figure 4.  $K_2CO_3$  specific gravity change diagram with vacuum degree.

### 4.1.3. EVM Particle Size

The main operations and data of KE2 series samples are shown in Table 3. For the composite material prepared by 0.4~0.8 mm EVM (E2), even with vacuum impregnation, the specific gravity of  $K_2CO_3$  is only 48.347 wt.%, which is lower than the KE1-4 sample (3~6 mm EVM:E1) of the same preparation process. It can be seen that the large-particle-size EVM can carry more  $K_2CO_3$ . From the microscopic level, the different content of  $K_2CO_3$  carried by EVM with different particle sizes should be related to EVM pore parameters. Therefore, the porosity and other parameters of E1 and E2 are measured by mercury intrusion porosimetry, and the MIP test results are shown in Table 4.

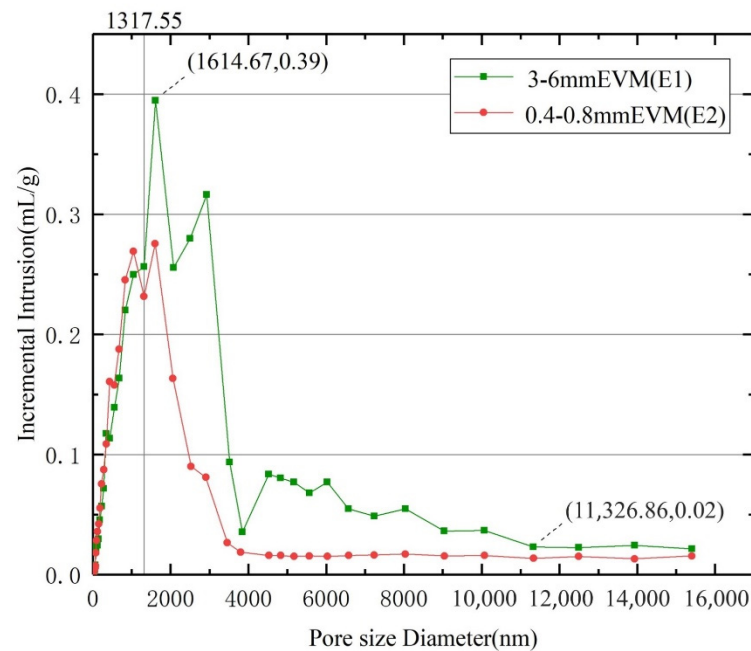
Table 3. KE2 series of major operations and sample data.

Sample No.	Vacuum Degree (Absolute Pressure) $P_{abs}/kPa$	Quality after Drying $m_{KE}/g$	$K_2CO_3$ Accounts for the Specific Gravity of Composite Material $\eta/wt. \%$
KE2-2	101.2	9.522	47.490
KE2-4	7.8	9.680	48.347

**Table 4.** MIP test results.

Sample No.	Porosity/%	Average Pore Diameter $D_A$ /nm	Total Pore Area $S$ /(m <sup>2</sup> /g)	Bulk Density $\rho_B$ /(g/cm <sup>3</sup> )
E1	96.2082	1068.24	18.418	0.1956
E2	98.4322	861.82	18.568	0.2460

Table 4 shows that both E1 and E2 have a high porosity of more than 95% and a total pore area of about 18.5 m<sup>2</sup>/g. However, the difference in average pore diameter values of them is larger. The average pore diameter of E1 is as high as 1068.24 nm, which is about 23.952% larger than E2. It can be seen that the pore diameter is the main factor that affects how much K<sub>2</sub>CO<sub>3</sub> the EVM carries. Figure 5 shows that within the pore size range of 1317.55 to 11,326.86 nm, the incremental intrusion of E1 is significantly higher than that of E2. As the data continue to rise, the incremental intrusion by E1 can reach as high as 0.39 mL/g, which is about 43.116% larger than E2. It can be seen that E1 has more pores with a pore diameter larger than 1317.55 nm. Under vacuum, E1 can absorb a large amount of K<sub>2</sub>CO<sub>3</sub> solution and obtain higher K<sub>2</sub>CO<sub>3</sub> specific gravity.

**Figure 5.** Incremental intrusion vs pore size.

Taking into account the difference in E1 and E2 bulk density ( $\rho_B$ , g/cm<sup>3</sup>), the ratio ( $\rho_{KE}$ , g/cm<sup>3</sup>) of K<sub>2</sub>CO<sub>3</sub> mass to EVM bulk volume is used to compare the salt content of composite materials with different particle sizes:

$$\rho_{KE} = \frac{m_{K_2CO_3}}{V_0} = \frac{m_{KE} - m_E}{m_E} \times \rho \quad (3)$$

where  $V_0$  is the bulk volume of EVM, cm<sup>3</sup>; and  $m_{K_2CO_3}$  is the mass of K<sub>2</sub>CO<sub>3</sub> in the composite material, g. It can be known from the calculation results of  $\rho_{KE}$  in Figure 6, the  $\rho_{KE}$  value of the KE2-2 sample prepared by the impregnation method is 0.222 g/cm<sup>3</sup>, which is about 1.18% larger than that of the KE1-2 sample. However, the  $\rho_{KE}$  value of the KE1-4 sample prepared by the vacuum impregnation method can reach 0.466 g/cm<sup>3</sup>, which is much higher than that of other samples. It can be seen that the composites prepared from large-particle-size EVM and K<sub>2</sub>CO<sub>3</sub> solutions in a vacuum environment can store more

inorganic salts. The higher the content of inorganic salt per unit volume, the more energy is absorbed, which is more conducive to improving the practicability of the material.

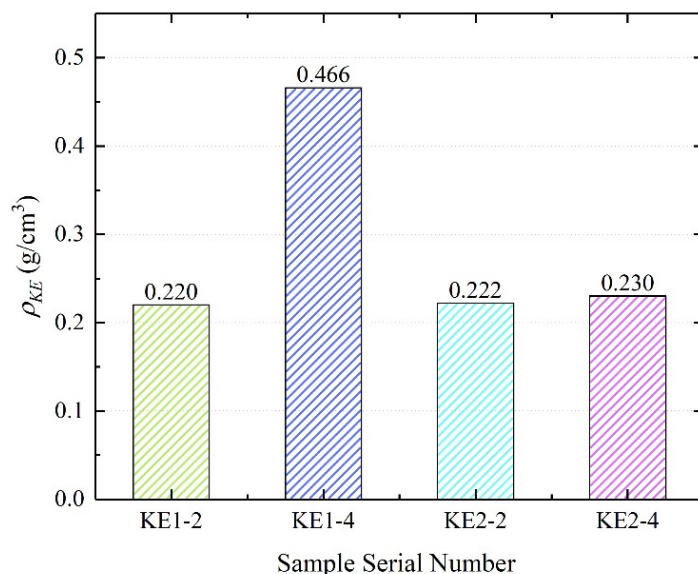


Figure 6. KE calculation result.

#### 4.1.4. Solution Concentration

Four K<sub>2</sub>CO<sub>3</sub> solutions of different concentrations are used to prepare K<sub>2</sub>CO<sub>3</sub>/EVM composite materials. The specific preparation data are shown in Figure 7. As the mass concentration of K<sub>2</sub>CO<sub>3</sub> solution increases, the specific gravity of K<sub>2</sub>CO<sub>3</sub> in the composite material gradually increases. The solution concentration of the KE3-3 sample is 0.103 g/mL higher than that of the previous sample, and the  $\eta$  difference between the two samples can reach 11.84 wt.%. The solution concentration of the KE3-4 sample is 0.417 g/mL higher than that of the KE3-3. However, the specific gravity of K<sub>2</sub>CO<sub>3</sub> only increased by 10 wt.%. It can be seen that the specific gravity of K<sub>2</sub>CO<sub>3</sub> in the composite material does not increase linearly with the increase of the solution concentration, instead, there is a trend of decreasing growth. This phenomenon is mainly because EVM absorbs K<sub>2</sub>CO<sub>3</sub> solution through capillary action, but the absorbing capacity of the capillarity will decrease with the increase of the concentration of the solution [25].

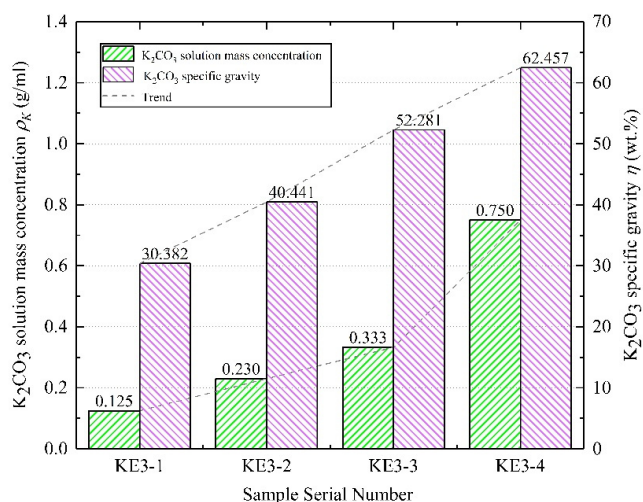


Figure 7. KE3 series samples preparation data.



## 4.2. Distribution of $K_2CO_3$

### 4.2.1. Vacuum Degree

The  $K_2CO_3$ /EVM composite material prepared by the vacuum impregnation method can carry more  $K_2CO_3$ . In order to study the distribution of  $K_2CO_3$  in the EVM of composite materials prepared in different environments, the EVM is used as a blank control to observe the surface and cross-sectional morphologies of KE1-2 and KE1-4 samples. The SEM images of the surface of EVM, KE1-2 and KE1-4 samples are shown in Figure 8. Figure 8a shows that in EVM without  $K_2CO_3$ , pores of different sizes are clearly visible on the surface. In contrast, in the KE1-2 sample prepared based on the impregnation method (Figure 8b), most of the space in the pores is occupied by  $K_2CO_3$  (dark), and only the outline of the pores (bright white) can be observed on the surface. The surface of the KE1-4 sample prepared by the vacuum impregnation method (Figure 8c) is covered by more  $K_2CO_3$ , and it is almost impossible to observe the pore profile. Magnifying the pore by 10.0k times, it is found that the pores are filled with a large amount of  $K_2CO_3$  (red circles in Figure 8d), and there are small gaps between  $K_2CO_3$  particles that can be used for water vapor medium circulation (blue rectangles).

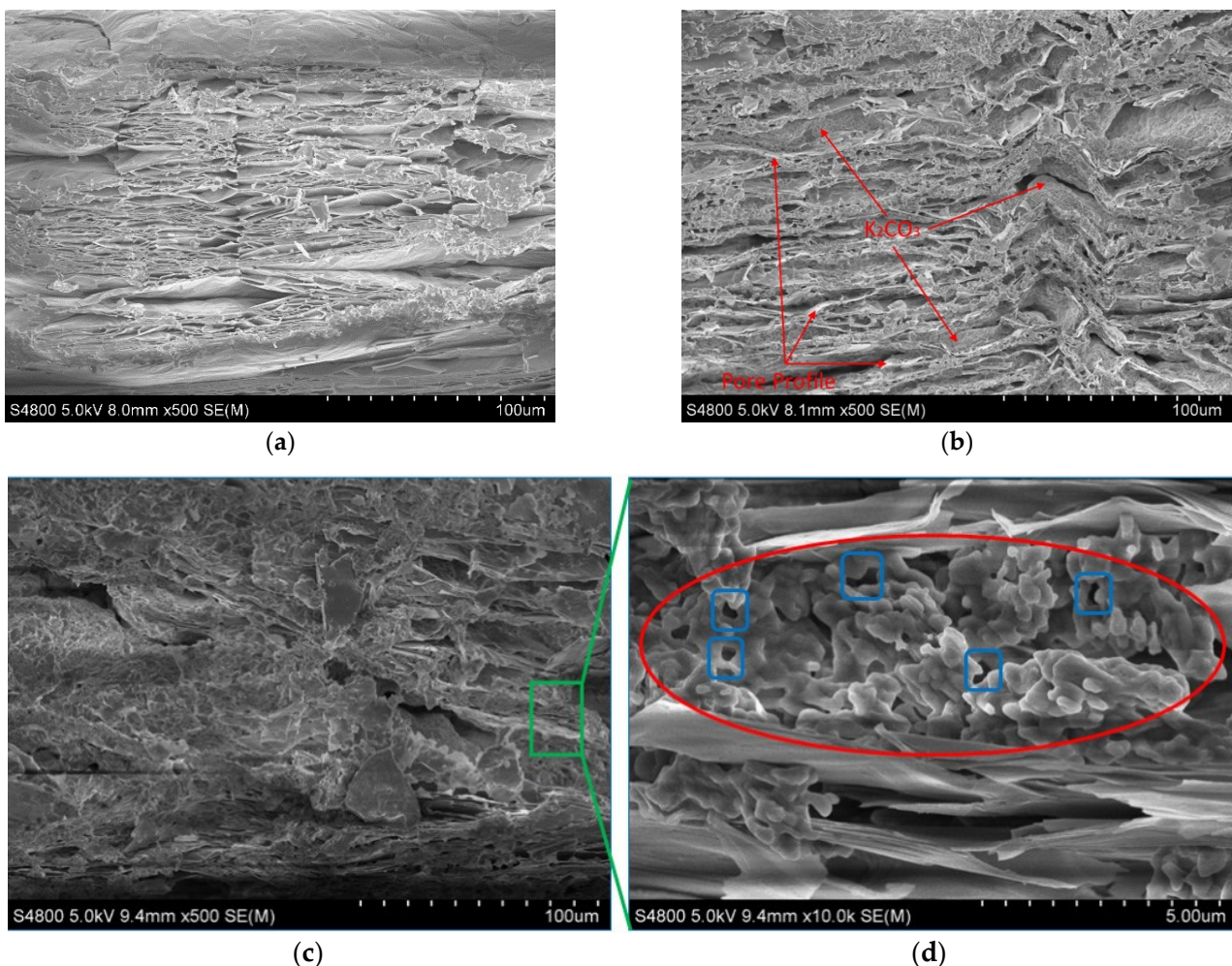


**Figure 8.** SEM images of EVM, KE1-2 and KE1-4 samples surfaces. (a) EVM; (b) KE1-2; (c) KE1-4; and (d) KE1-4 Porosity.

The SEM images of the cross-sections of EVM, KE1-2 and KE1-4 samples are shown in Figure 9. The lamellas in the EVM section are thin and dense (Figure 9a), and there are random connections between the lamellas that form pores of different sizes. Only a small number of pores in the cross-section of the prepared KE1-2 sample contain  $K_2CO_3$ , while

the observed  $K_2CO_3$  coverage areas at the section of the KE1-4 sample are more (red circles in Figure 9b,c). Although the KE1-4 sample carries a large amount of  $K_2CO_3$ , there are also many unfilled pores inside. Among the pores containing  $K_2CO_3$  in the KE1-4 sample, most of the  $K_2CO_3$  in the large pores adhered to the wall of the pore, and the small pores are basically filled with  $K_2CO_3$ . The  $K_2CO_3$  in the small pores is in the form of particles, and the medium circulation gap between the particles is not large.

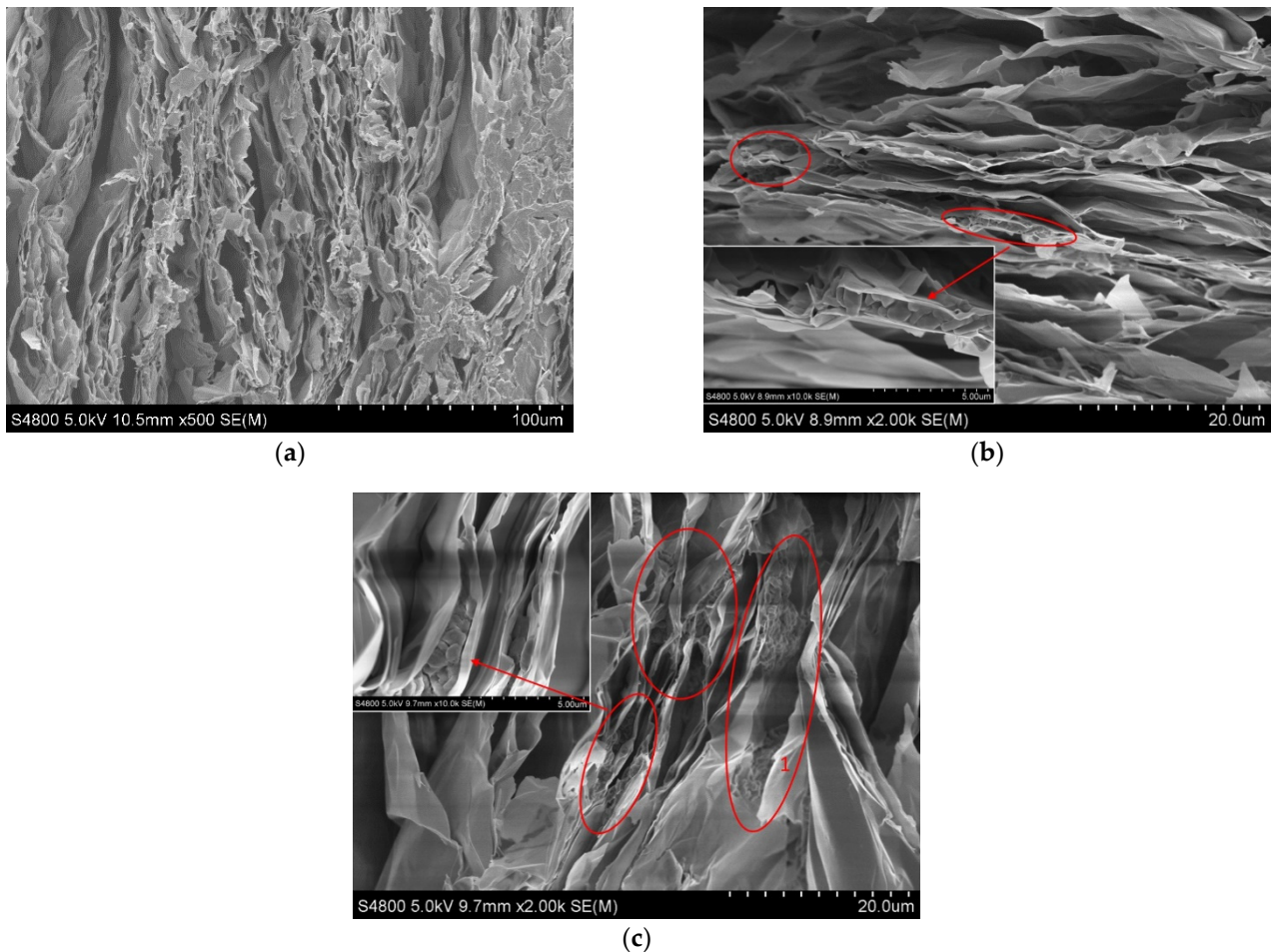


**Figure 9.** SEM images of EVM, KE1-2 and KE1-4 samples cross-sections. (a) EVM; (b) KE1-2; and (c) KE1-4.

#### 4.2.2. Solution Concentration

The SEM images of the cross-section of the KE3 series are shown in Figure 10. Figure 10 shows that although the concentration of the solution changes during the preparation of the composite material, the  $K_2CO_3$  in the macropores of the KE3 series samples adheres more to the wall of the pores, leaving a larger medium flow area (blue rectangles), and it is similar to the morphology in the macropores of the KE1-4 sample (1 in Figure 9c). The distribution of  $K_2CO_3$  in the small pores has also not changed with the different concentrations of the solution, and it is basically filled (red circles). It can be seen that the morphology of  $K_2CO_3$  in the pores of the composite material will not change significantly with the decrease in the solution concentration. Using a high-concentration solution to prepare composite materials can make the EVM carry more  $K_2CO_3$  and improve the practicability of the material.

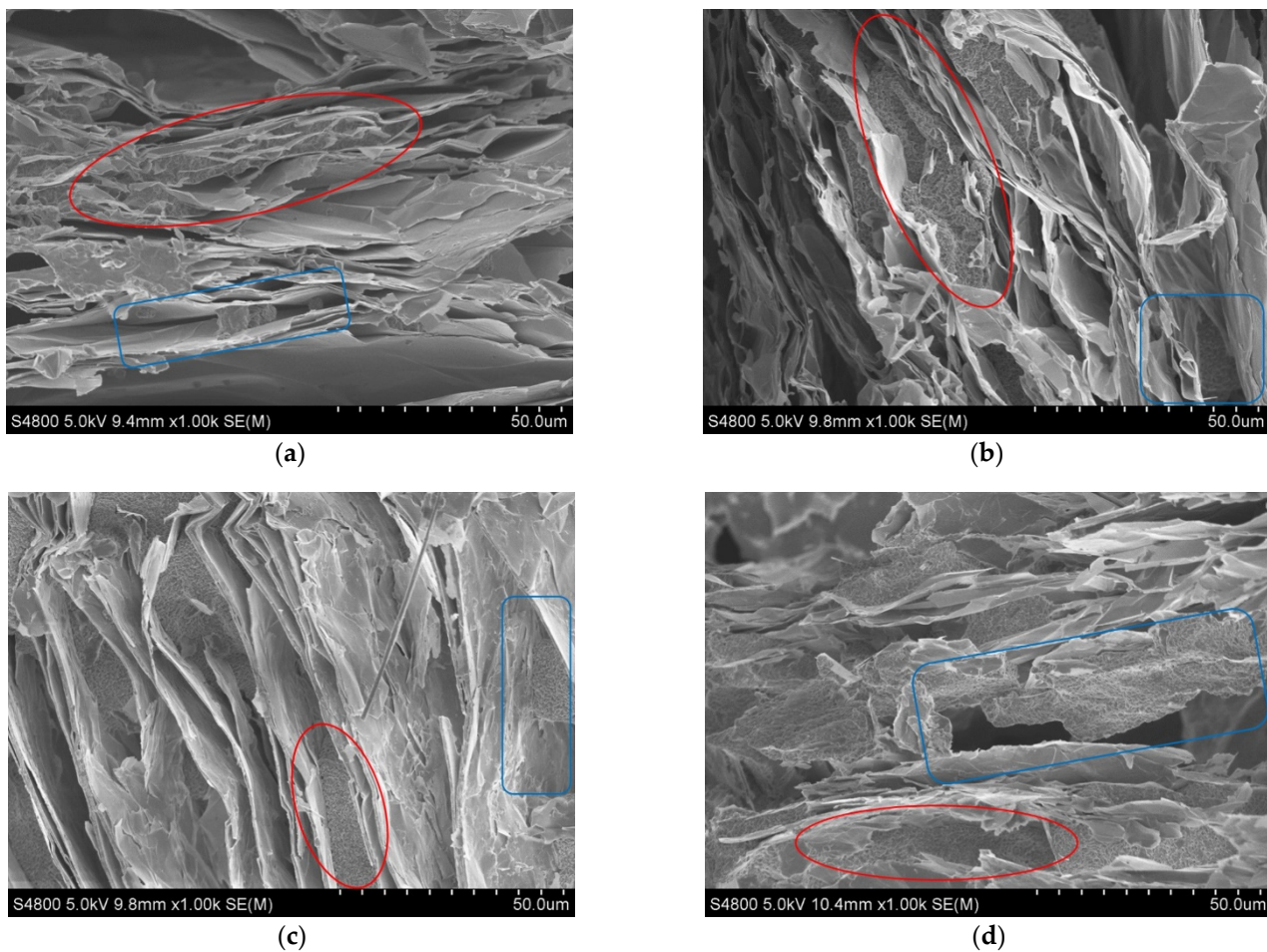


**Figure 10.** SEM image of KE3 series sample cross-section. (a) KE3-1; (b) KE3-2; (c) KE3-3; and (d) KE3-4.

## 5. Conclusions

$K_2CO_3$ /EVM composite material, as one of many substances in thermochemical adsorption energy storage technology, has outstanding advantages such as low price, non-corrosiveness and toxicity. Its dehydration temperature is lower than  $120\text{ }^\circ\text{C}$ , which is very suitable for use with solar thermal utilization technology. In order to obtain a more practical composite material, based on the impregnation method and the vacuum impregnation method, the influence of the preparation process, the particle size of the expanded vermiculite and the solution concentration on the  $K_2CO_3$ /EVM composite material are studied, and the conclusions are as follows:

The vacuum degree is the main factor in order to increase the specific gravity of  $K_2CO_3$ . When the vacuum degree is lower than 60 kPa, the specific gravity of  $K_2CO_3$  in the composite material is stable at about 53 wt.%, and there is no significant change. When the vacuum degree is higher than 60 kPa, the specific gravity of  $K_2CO_3$  in the composite material shows an upward trend with the increase of the vacuum degree, up to 70.440 wt.% (the vacuum degree is 6.7 kPa).

Large-particle-size EVM can carry more  $K_2CO_3$ . As 3~6 mm EVM (E1) has more large pores with pore diameters of 1317.55~11,326.86 nm, E1 can absorb more  $K_2CO_3$  solution than E2 (0.4~0.8 mm EVM). Among the samples, the  $K_2CO_3$  content per cubic centimeter of the KE1-4 sample prepared by E1 can be as high as 0.466 g.

Part of the pores in the composite material does not contain  $K_2CO_3$  particles. Among the pores containing  $K_2CO_3$ , the  $K_2CO_3$  in the large pores is more adhered to the wall of the pore, while the small pores are basically filled with  $K_2CO_3$ . Under the effect of

vacuum, more  $K_2CO_3$  is distributed on the surface and inside of the EVM, as a result, the composite material has a higher specific gravity of  $K_2CO_3$ . The increase in the concentration of the impregnating solution promotes the increase of the specific gravity of  $K_2CO_3$  in the composite material, but the distribution of  $K_2CO_3$  particles in the pores does not change.

**Author Contributions:** Conceptualization, D.Z.; Data curation, X.Y. and T.H.; Writing—original draft, D.Z., J.D. and D.B.; Writing—review & editing, X.Y. and T.H. All authors have read and agreed to the published version of the manuscript.

**Funding:** This research received no external funding.

**Institutional Review Board Statement:** Not applicable.

**Informed Consent Statement:** Not applicable.

**Data Availability Statement:** The data presented in this study are available on request from the corresponding author.

**Conflicts of Interest:** The authors declare no conflict of interest with respect to the research, authorship, and/or publication of this article.

## References

1. IPCC. *Global Warming of 1.5°C. An IPCC Special Report on the Impacts of Global Warming of 1.5°C Above Pre-Industrial Levels and Related Global Greenhouse Gas Emission Pathways, in the Context of Strengthening the Global Response to the Threat of Climate Change, Sustainable Development, and Efforts to Eradicate Poverty*; IPCC: Geneva, Switzerland, 2018.
2. IPCC. *Climate Change 2014: Mitigation of Climate Change. Contribution of Workinggroup III to the Fifth Assessment Report of the Intergovernmental Panel on Climate Change*; Edenhofer, O., Pichs-Madruga, R., Sokona, Y., Farahani, E., Kadner, S., Seyboth, K., Adler, A., Baum, I., Brunner, S., Eickemeier, P., et al., Eds.; Cambridge University Press: Cambridge, UK; New York, NY, USA, 2014.
3. Michel, B.; Mazet, N.; Neveu, P. Experimental investigation of an open thermochemical process operating with a hydrate salt for thermal storage of solar energy: Local reactive bed evolution. *Appl. Energy* **2016**, *180*, 234–244. [[CrossRef](#)]
4. Donkers, P.A.J.; Sögütoglu, L.C.; Huinink, H.P.; Fischer, H.R.; Adan, O.C.G. A review of salt hydrates for seasonal heat storage in domestic applications. *Appl. Energy* **2017**, *199*, 45–68. [[CrossRef](#)]
5. Shkatulov, A.I.; Houben, J.; Fischer, H.; Huinink, H.P. Stabilization of  $K_2CO_3$  in vermiculite for thermochemical energy storage. *Renew. Energy* **2020**, *150*, 990–1000. [[CrossRef](#)]
6. Gaeini, M.; Shaik, S.A.; Rindt, C.C.M. Characterization of potassium carbonate salt hydrate for thermochemical energy storage in buildings. *Energy Build.* **2019**, *196*, 178–193. [[CrossRef](#)]
7. Yu, N.; Wang, R.Z.; Lu, Z.S.; Wang, L.W. Development and characterization of silica gel–LiCl composite sorbents for thermal energy storage. *Chem. Eng. Sci.* **2014**, *111*, 73–84. [[CrossRef](#)]
8. Courbon, E.; D’Ans, P.; Skrylnyk, O.; Frere, M. New prominent lithium bromide-based composites for thermal energy storage. *J. Energy Storage* **2020**, *32*, 101699. [[CrossRef](#)]
9. Posern, K.; Kaps, C. Calorimetric studies of thermochemical heat storage materials based on mixtures of  $MgSO_4$  and  $MgCl_2$ . *Thermochim. Acta* **2010**, *502*, 73–76. [[CrossRef](#)]
10. Shere, L.; Trivedi, S.; Roberts, S.; Sciacovelli, A.; Ding, Y. Synthesis and Characterization of Thermochemical Storage Material Combining Porous Zeolite and Inorganic Salts. *Heat Transf. Eng.* **2019**, *40*, 1176–1181. [[CrossRef](#)]
11. Chan, K.C.; Chao, C.Y.; Sze-To, G.N.; Hui, K.S. Performance predictions for a new zeolite 13X/ $CaCl_2$  composite adsorbent for adsorption cooling systems. *Int. J. Heat Mass Transf.* **2012**, *55*, 3214–3224. [[CrossRef](#)]
12. Grekova, D.; Gordeval, G.; Aristovy, I. Composite “LiCl/vermiculite” as advanced water sorbent for thermal energy storage. *Appl. Therm. Eng.* **2017**, *124*, 1401–1408. [[CrossRef](#)]
13. Veselovskaya, J.V.; Critoph, R.E.; Thorpe, R.N.; Metcalf, S.; Tokarev, M.M.; Aristov, Y.I. Novel ammonia sorbents “porous matrix modified by active salt” for adsorptive heat transformation: 3. Testing of “BaCl<sub>2</sub>/vermiculite” composite in a lab-scale adsorption chiller. *Appl. Therm. Eng.* **2010**, *30*, 1188–1192. [[CrossRef](#)]
14. Zhang, Y.N.; Wang, R.Z.; Zhao, Y.J.; Li, T.X.; Riffat, S.B.; Wajid, N.M. Development and thermochemical characterizations of vermiculite/SrBr<sub>2</sub> composite sorbents for low-temperature heat storage. *Energy* **2016**, *115*, 120–128. [[CrossRef](#)]
15. Li, C. *Preparation and Property Control of Mineral-based Composite Thermal Storage Materials*; Central South University: Changsha, China, 2013.
16. Xu, B.; Ma, H.; Lu, Z.; Li, Z. Paraffin/expanded vermiculite composite phase change material as aggregate for developing lightweight thermal energy storage cement-based composites. *Appl. Energy* **2015**, *160*, 358–367. [[CrossRef](#)]
17. Karaipekli, A.; Sarı, A. Preparation, thermal properties and thermal reliability of eutectic mixtures of fatty acids/expanded vermiculite as novel form-stable composites for energy storage. *J. Ind. Eng. Chem.* **2010**, *16*, 767–773. [[CrossRef](#)]
18. Tian, W. *Study on Design, Synthesis and Properties of Vermiculite Composite Functional Materials*; Beijing University of Chemical Technology: Beijing, China, 2017.

19. Feng, J.; Liu, M.; Fu, L.; Zhang, K.; Xie, Z.; Shi, D.; Ma, X. Enhancement and mechanism of vermiculite thermal expansion modified by sodium ions. *RSC Adv.* **2020**, *10*, 7635–7642. [[CrossRef](#)] [[PubMed](#)]
20. de Vargas Brião, G.; da Silva, M.G.C.; Vieira, M.G.A. Neodymium recovery from aqueous solution through adsorption/desorption onto expanded vermiculite. *Appl. Clay Sci.* **2020**, *198*, 105825. [[CrossRef](#)]
21. Sutcu, M. Influence of expanded vermiculite on physical properties and thermal conductivity of clay bricks. *Ceram. Int.* **2015**, *41 Pt B*, 2819–2827. [[CrossRef](#)]
22. Koksall, F.; Mutluay, E.; Gencel, O. Characteristics of isolation mortars produced with expanded vermiculite and waste expanded polystyrene. *Constr. Build. Mater.* **2020**, *236*, 117789. [[CrossRef](#)]
23. Mazloomi, F.; Jalali, M. Effects of vermiculite, nanoclay and zeolite on ammonium transport through saturated sandy loam soil: Column experiments and modeling approaches. *Catena* **2019**, *176*, 170–180. [[CrossRef](#)]
24. Sögütöglü, L.C.; Donkers, P.A.J.; Fischer, H.R.; Huinink, H.P.; Adan, O.C.G. In-depth investigation of thermochemical performance in a heat battery: Cyclic analysis of  $K_2CO_3$ ,  $MgCl_2$  and  $Na_2S$ . *Appl. Energy* **2018**, *215*, 159–173. [[CrossRef](#)]
25. Wang, C.; Zhang, P.; Xie, C.Q.; Wu, H. Effect of Different Concentration Salt Solution and Saline Soil on Capillary Water Upward Movement. *Water Sav. Irrig.* **2014**, *12*, 26–28.